Int. J. Nanosci. Nanotechnol., Vol. 17, No. 3, Sept. 2021, pp. 181-190

Viscous Dissipation Effect on Micro Nanofluid in the Presence of Inclined Magnetic Field

G. Narender[1,*] and K. Govardhan[2]

[1]Department of Humanities & Sciences (Mathematics), CVR College of Engineering, Hyderabad, Telangana State, India
[2]Department of Mathematics, GITAM University, Hyderabad, Telangana State, India

(*) Corresponding author: gnriimc@gmail.com
(Received: 26 March 2020 and Accepted: 26 July 2021)

Abstract

The aim of the present study is to investigate the effects of viscous dissipation and chemical reaction on stagnation point flow of electrical magnetohydrodynamic (EMHD) field over stretching sheet by considering micro nanofluid. Contribution of magnetic field is considered in the flow field, whereas the heat convection is associated with the Brownian motion, thermophoresis and viscous dissipation and chemical reaction is incorporated in the mass diffusion. The problem is governed by coupled non-linear Partial Differential Equations (PDE) with appropriate boundary conditions. The transformed non-dimensional and coupled governing Partial Differential Equations are solved numerically using Adam's – Moulton method along with shooting technique. The effects of the various dimensionless parameters entering the problem on velocity, microrotation, temperature, and concentration fields are studied.

Keywords: *EMHD, Micro nano fluid, Stretching sheet, Viscous dissipation, Chemical reaction.*

1. INRODUCTION

The analysis on Stagnation nano energy conversion problem of steady nanofluids flows over a stretching sheet has been of increasing importance over the last few years. Qualitative analyses of studies have notable bearing on several industrial applications, especially polymer sheet extrusion from a dye, drawing of plastic films, etc. These processes require cooling of the stretching sheet during the manufacturing stages at very high temperature. There are some techniques of cooling the stretching surface. The present investigation considers nanofluid as necessary for more effective cooling of the stretching surface.

MHD stagnation point flow of micropolar fluid towards a moving sheet has been analyzed numerically by Ashraf and Bashir [1]. Rauf et al. [2] investigated numerical solution of the problem of MHD flow of micropolar fluid over a stretchable sheet. Rashidi et al. [3] further advanced the analysis of [1] to consider the effects of mixed convection to the problem.

Analytical technique based on HAM to the problem of unsteady micropolar fluid and heat transfer influenced by a stretching sheet was studied by Shehzad et al. [4]. Pal et al. [5] studied stagnation point radiative flow of nanofluid over a surface with porous medium and Pal and Mandal [6] extended the problem with mixed convective nanofluid flow with chemical reaction. Hayat et al. [7] have studied effect of chemical reaction on mixed convective flow over a stretching surface. Hayat et al. [8] studied MHD 3D flow of nanofluid in presence of convective conditions. The types of flow problems under convective surface conditions have been examined by Hayat et al. [9]. Imtiaz et al. [10] explored Hall and radial magnetic field effects on radiative peristaltic flow of Carreau-Yasuda fluid in a channel with convective heat and mass transfer. Hayat et al. [11] analyzed the convective heat and mass transfer in flow by an inclined stretching cylinder. M. Sheikholeslami et al. [12] presented

modification for helical turbulator to augment heat transfer behavior of nanomaterial via numerical approach. A triplex-tube heat exchanger with tree-like and rectangular fins along with hybrid nanoparticles made of $MoS_2 - TiO_2$ are put into perspective to dispose of this weakness and Galerkin Finite Element Method (GFEM) is applied using Flex PDE to analyze the solidification process and evaluate the influence of single and combined usage of fins and nanoparticles was studied by Kh. Hosseinzadeh et al. [13]. Kh. Hosseinzadeh et al. [14] demonstrated the effects of the radiation parameter, porosity and the magnetic parameter have been analyzed on temperature distribution and fluid flow streamlines and on the local and average Nusselt numbers. Kh. Hosseinzadeh et al. [15] thoroughly studied Phase change materials (PCMs) are of great importance regarding saving energy, however, their low thermal conductivity lengthens the transition evolution which is the main problem of this system. K. Govardhan et al. [16] talked about the impact of viscous dissipation on MHD flow passing over a stretching sheet. Several researchers have contributed in the study of the stagnation point MHD flow in the light of various significant effects [17-22].

Recently A. Rauf et al. [23] studied the MHD stagnation point flow of micro nanofluid towards a stretching sheet with convective and zero mass flux conditions. Objective of the present investigation is to extend analysis of A. Rauf et al. [23] by taking viscous dissipation. This study finds numerical solution for MHD stagnation point flow with viscous dissipation.

2. PROBLEM FORMULATION

To construct the model, consider a two-dimensional incompressible stagnation flow of electrically conducting micro nanofluid past a stretching sheet. The origin is located at the slit through which is drawn through the fluid medium, the $x-$ axis is chosen along the stretching sheet and $y-$ axis is taken normal to it. The fluid motion within the film is due to a slip boundary layer for stretching sheet. The associated equations for the flow model are given in (1)-(5), which under boundary layer approximation can be written as [23],

$$\frac{\partial u}{\partial x}+\frac{\partial v}{\partial y}=0, \tag{1}$$

$$\left.\begin{aligned}\rho\left(u\frac{\partial u}{\partial x}+v\frac{\partial u}{\partial y}\right)=U\frac{dU}{dx}+\\ \left(\mu+k\frac{\partial^2 u}{\partial y^2}\right)+k\frac{\partial \upsilon}{\partial y}+\sigma_e B_0^2\left(U-u\right)\end{aligned}\right\}, \tag{2}$$

$$\left.\begin{aligned}\rho j\left(u\frac{\partial \upsilon}{\partial x}+v\frac{\partial \upsilon}{\partial y}\right)=\gamma\frac{\partial^2 \upsilon}{\partial y^2}-\\ k\left(2\upsilon+\frac{\partial u}{\partial y}\right)\end{aligned}\right\}, \tag{3}$$

$$\left.\begin{aligned}u\frac{\partial T}{\partial x}+v\frac{\partial T}{\partial y}=\mu\left(\frac{\partial u}{\partial y}\right)^2+\alpha\frac{\partial^2 T}{\partial y^2}+\\ \tau\left[D_B\frac{\partial T}{\partial y}\frac{\partial C}{\partial y}+\frac{D_T}{T_\infty}\left(\frac{\partial T}{\partial y}\right)^2\right]\end{aligned}\right\}, \tag{4}$$

$$\left.\begin{aligned}u\frac{\partial C}{\partial x}+v\frac{\partial C}{\partial y}=D_B\frac{\partial^2 C}{\partial y^2}+\frac{D_T}{T_\infty}\frac{\partial^2 T}{\partial y^2}-\\ k_0\left(C-C_\infty\right)\end{aligned}\right\}, \tag{5}$$

The associated boundary conditions for the above system of equations are,

$$\left\{\begin{aligned}&u\left(x,0\right)=b\,x, v\left(x,0\right)=0, \upsilon\left(x,0\right)=0,\\ &-k\frac{\partial T}{\partial y}=h_f\left(T_f-T\right),\\ &D_B\frac{\partial C}{\partial y}+\frac{D_B}{T_\infty}\frac{\partial T}{\partial y}=0,\\ &u\left(x,\infty\right)=U=a\,x,\ \upsilon\left(x,\infty\right)=0,\\ &T\left(x,\infty\right)=T_\infty,\ C\left(x,\infty\right)=C_\infty\end{aligned}\right. \tag{6}$$

where $b<0$ corresponds to the shrinking rate, σ_e is the electrical conductivity of the fluid, α is the thermal diffusivity, of the fluid, υ is the microrotation, ρ is the density, p is the pressure, μ is the viscosity, k is the vortex viscosity, j is the microinertia density, γ is the spin gradient viscosity, $\tau=\frac{\left(\rho C\right)_p}{\left(\rho C\right)_f}$ is the ratio of

nanoparticle heat capacity coefficient, D_T is the thermophoretic coefficient, D_B is the Brownian diffusion coefficient, h_f is the heat transfer coefficient, and k_0 is the chemical reaction coefficient.

In this portion we convert the system of (1)–(5) along with the boundary conditions (6) into a unitless form. To find out the solution of PDEs we use the following similarity transformation:
The similarity variable is defined as:

$$\eta = y\sqrt{\frac{a}{\upsilon}} \tag{7}$$

The temperature and concentration dimensionless functions $\theta(\eta)$, $\beta(\eta)$ and dimensionless stream function ψ are given in the form of

$$\left.\begin{aligned} g(\eta) &= \frac{\upsilon}{U},\ \theta(\eta) = \frac{T - T_\infty}{T_f - T_\infty}, \\ \beta(\eta) &= \frac{C - C_\infty}{C_\infty},\ \psi = \sqrt{a\nu x}\ f(\eta). \end{aligned}\right\} \tag{8}$$

The stream function $\psi = \psi(x, y)$ is identically satisfying continuity equation. Mathematically,

$$u = \frac{\partial \psi}{\partial y},\ v = -\frac{\partial \psi}{\partial x}. \tag{9}$$

Using similarity transformation from Eqs. (8) – (9) in momentum Eq. (2), energy Eq. (4) and concentration Eq. (5) along the boundary conditions (6), we get the following ODEs.

$$\left.\begin{aligned} (1+B)\, f''' - B\, g' - \left(f'\right)^2 + f\, f'' + \\ M^2\left(1 - f'\right) + 1 = 0 \end{aligned}\right\}, \tag{10}$$

$$\left.\begin{aligned} C\, g'' + AR\left(f'' - 2g\right) - f'\, g + \\ f\, g' = 0 \end{aligned}\right\}, \tag{11}$$

$$\left.\begin{aligned} \frac{\theta''}{\Pr} + f\,\theta' + Nb\,\theta'\,\beta' + Nt\left(\theta'\right)^2 + \\ Ec\left(f''\right)^2 = 0 \end{aligned}\right\}, \tag{12}$$

$$\beta'' + Sc\, f\, \beta' + \frac{Nt}{Nb}\theta'' - Sc\, k_1\, \beta = 0. \tag{13}$$

The transformed boundary conditions are:

$$\left.\begin{aligned} &f'(0) = N,\ f(0) = 0,\ g(0) = 0, \\ &\theta'(0) = -Bi\left(1 - \theta(0)\right), \\ &Nt\,\theta'(0) + Nb\,\beta'(0) = 0, \\ &f'(\infty) = 1,\ g(\infty) = 0, \\ &\theta(\infty) = 0,\ \beta(\infty) = 0. \end{aligned}\right\} \tag{14}$$

where $M = \sqrt{\frac{\sigma B_0^2}{\rho a}}$ denotes the magnetic parameter, $A = \frac{\mu}{\rho j a}$ microinertia density parameter, $B = \frac{k}{\mu}$ is vortex viscosity parameter, $C = \frac{\gamma}{\mu j}$ the spin gradient parameter, $\Pr = \frac{\nu}{\alpha}$, the Prandtl number, $Nb = \frac{(\rho C)_p D_B (C_\infty)}{(\rho C)_f \alpha}$ the Brownian motion parameter, $Nt = \frac{(\rho C)_p D_T (T_w - T_\infty)}{(\rho C)_f \alpha T_\infty}$ the thermophoresis parameter, $Ec = \frac{u_w^2}{(\rho C)_f (T_w - T_\infty)}$ is the Eckert number, $k_1 = \frac{k_0}{a}$ is the chemical reaction parameter, $Bi = \frac{h_f}{k}\sqrt{\frac{\nu}{a}}$ Biot number, $Sc = \frac{\nu}{D_B}$ the Schmidt number and $N = \frac{b}{a}$ is the shrinking parameter.

3. NUMERICAL COMPUTATION

The shooting technique requires the initial guess for $f''(\eta), g'(\eta), \theta(\eta)$ and $\beta(\eta)$ at $\eta = 0$ and through Newton's method we vary each guess until we obtain an appropriate solution for our problem. To check accuracy of the obtained numerical results by Shooting technique

we compare them by the numerical results acquired by A. Rauf et al. [23] and found them in excellent agreement. The analytic solution of the system of equations with corresponding boundary conditions Eqs. (10)–(14) cannot be found because they are nonlinear and coupled. The governing Partial Differential Equation are transformed into Ordinary Differential Equation using similarity transformations. The numerical solution for the system of differential equation are developed using Adam's – Moulton method of order four along with shooting technique. In order to solve the system of Ordinary Differential Equations with boundary conditions equations.

Let $f = y_1, y_1' = y_2, y_2' = y_3,$ then.

$$f''' = y_3' = \frac{\begin{pmatrix} -y_1 y_3 + (y_2)^2 - 1 + R y_5 \\ -M^2 (1 - y_2) \end{pmatrix}}{(1+R)}, \quad (15)$$

$g = y_4, y_4' = y_5,$ then

$$g'' = y_5' = \frac{\begin{pmatrix} -R\ A(y_3 - 2y_4) + \\ y_2 y_4 - y_1 y_5 \end{pmatrix}}{C}, \quad (16)$$

$\theta = y_6, y_6' = y_7,$ then

$$y_7' = \theta'' = -\Pr\begin{pmatrix} y_1 y_7 + Nb\, y_7\, y_9 + \\ Nt(y_7)^2 + Ec(y_3)^2 \end{pmatrix}, \quad (17)$$

$\beta = y_8, y_8' = y_9,$ then

$$y_9' = \beta'' = \frac{\Pr Nt}{Nb}\begin{bmatrix} y_1 y_7 + Nb\, y_7\, y_9 + \\ Nt(y_7)^2 + Ec(y_3)^2 \end{bmatrix} + Sc\, k_1\, y_8 - Sc\, y_1\, y_9, \quad (18)$$

with the boundary conditions

$$\left.\begin{array}{l} y_1(0) = 0,\ y_2(0) = N,\ y_3(0) = a_1, \\ y_4(0) = 0, y_5(0) = a_2,\ y_6(0) = a_3, \\ y_7(0) = Bi(1 - a_3), y_8(0) = a_4, \\ y_9(0) = \dfrac{Nt}{Nb}(1 - a_3), y_9(\infty) = 1, \\ y_4(\infty) = 0,\ y_6(\infty) = 0,\ y_8(\infty) = 0. \end{array}\right\} \quad (19)$$

In the above system of equations, the missing initial conditions a_1, a_2, a_3 and a_4 are to be chosen such that.

$$\left.\begin{array}{l} y_3(\eta_\infty, a_1, a_2, a_3, a_4) = 0; \\ y_5(\eta_\infty, a_1, a_2, a_3, a_4) = 0; \\ y_6(\eta_\infty, a_1, a_2, a_3, a_4) = 0; \\ y_8(\eta_\infty, a_1, a_2, a_3, a_4) = 0; \end{array}\right\} \quad (20)$$

The shooting technique requires the initial guess for a_1, a_2, a_3 and a_4 by the Newton's mechanism we update each guess until we obtain an approximate result for our problem. To strengthen the reliability of the obtained numerical results by the shooting technique. The choice of $\eta_\infty = 10$ was more than enough for end condition. The convergence criteria are chosen to be successive value agree up to 3 significant digits.

4. RESULTS AND DISCUSSION

To get the physical insight into the problem, the results are discussed through graphs. Numerical results are obtained by fixed $A = 0.4,\ B = 2.0,\ C = 0.2,\ M = 0.5,$ $Ec = 0.1, k_1 = 0.1, \Pr = Nb = Nt = 0.3, Bi = 0.4,$ $Sc = 0.2$ and $N = -0.25$ all the graphs therefore correspond to these values unless specifically indicated on the appropriate graph. We adjusted $\eta_\infty = 6,10$ to have asymptotic behavior of velocity, microrotation, temperature, and concentration profiles.

In order to assess the accuracy of the numerical results, the present results are compared with the previous results. The temperature, and concentration profiles are compared with the available solution of A. Rauf et al. [23] in Table 1 and 2. It is observed that the present results are in good agreement with that of A. Rauf et al. [23].

Table 3 below shows the values of local Nusselt number $-\theta'(\eta)$ and local Sherwood number $-\beta'(\eta)$ when various values of all parameters involved are considered.

In Figure 1, it is observed that as the magnetic field produces a frictional force called the Lorentz force, which offers a resistance in a flow field, and due to its

Table 1. *Comparison of numerical values of Heat transfer rate at the sheet for different values of* $\Pr$ *and* Bi.

Pr	*Bi*	$-\theta'(0)$	
		A Rauf et al. [23]	**Present Study**
0.1	0.4	0.13516	0.13040920
0.2		0.15499	0.15427720
0.3		0.16835	0.16824340
0.5		0.18529	0.18529280
0.3	0.1	0.07444	0.07442008
	0.2	0.11853	0.11847930
	0.4	0.16835	0.16824360
	1.0	0.22502	0.22483410

Table 2*. Comparison of numerical values of Mass transfer rate at the sheet for different values of* $Sc, Nt, Nb,$ *and* k_1.

Sc	*Nt*	*Nb*	k_1	$-\beta'(0)$	
				A Rauf et al. [23]	**Present Study**
0.1	0.3	0.3	0.2	0.16848	0.16837800
0.2				0.16835	0.16824550
0.4				0.16817	0.16816840
0.8				0.16794	0.17276440
0.2	0.1	0.3	0.2	0.05619	0.05615552
	0.2			0.11231	0.11223740
	0.3			0.16835	0.16824560
	0.4			0.22432	0.22417970
0.2	0.3	0.1	0.2	0.50505	0.50473660
		0.2		0.25252	0.25236790
		0.3		0.16835	0.16824530
		0.4		0.12626	0.12618400
0.2	0.3	0.3	-0.1	0.16862	0.16850670
			0.1	0.16842	0.16193550
			0.5	0.16818	0..16807470
			1.0	0.16798	0.16787450

Table 3*. Numerical values of Heat transfer rate* $-\theta'(0)$ *and Mass transfer rate* $-\beta'(0)$ *for different values of* $M, \Pr, Bi, Nt, Nb,\ Sc, k_1$ *and* Ec *when* $A = 0.4, B = 2.0, C = 0.2,$ $N = -0.25,\ M = 0.5, \Pr = 0.3,\ Bi = 0.4, Sc = 0.2, k_1 = 0.2, Ec = 0.1.$

Nt	*Nb*	$-\theta'(0)$	$-\beta'(0)$
0.1	0.3	0.15539540	-0.05179846
0.2		0.15526200	-0.10350800
0.3		0.15512830	-0.15512830
0.4		0.15499370	-0.20665830
0.3	0.1	0.15512820	-0.46538470
	0.2	0.15512820	-0.23269230
	0.3	0.15512830	-0.15512830
	0.4	0.15512800	-0.11634600

velocity, the boundary layer pushes towards the wall of the sheet. An increase in the magnetic parameter causes a reduction in microrotation profiles, as described in Figure 2.

From Figure 3, it is observed that an increase in the Prandtl number results a decrease of the thermal boundary layer thickness and in general lower average temperature within the boundary layer. The reason is that smaller values of Pr are equivalent to increasing the thermal conductivities, and therefor heat can diffuse away from the heat surface more rapidly than for higher values of Pr .

Figure 4 describes the nature of Biot number *Bi* on temperature profile. It is detected that temperature is an increasing function of *Bi* . Physically, the rate of convective heat transport from the hot convectional liquid below the sheet to the liquid above the sheet intensifies.

Figure 5 is sketched to investigate the impact of *Ec* on fluid temperature. Generally, high viscous dissipative flow releases heat energy. So, we detect that an inflation in *Ec* is to enhance the temperature field. Moreover, we observed a notable effect on $\theta(\eta)$ with a growth in viscous dissipation parameter.

Figures 6 depict the influence of the Eckert number on the distributions of dimensionless concentration profile. While the intensity of viscous dissipation, as measured by the Eckert number strongly influences the temperature distribution (fig. 5), its impact on the concentration profile $(\beta(\eta))$ (fig. 6) is relatively weak. Physically, the Eckert number depicts the relation between the kinetic energy of the fluid particles and the boundary layer enthalpy. The kinetic energy of the fluid particles increases for higher values of *Ec*. Hence, the temperature of the fluid rises marginally and therefore, the associated momentum and thermal boundary layer thickness are enhanced.

Figure 7 shows that the variation in concentration profiles for different values of thermophoresis parameter *Nt* . It is noticeable that concentration profiles within the boundary layer increase with an increase in thermophoresis parameter.

Figure 8 display the Brownian motion parameter (Nb) on the concentration profile, as Brownian motion parameter increases the nanoparticle volume boundary layer thickness decreases. This happens because, as the value of *Nb* rises, the movement of the nanoparticles increases significantly, increasing the kinetic energy of the nanoparticles.

Figure 9 illustrates the effect of the Schmidt number on the concentration profile. It is observed that the concentration decreases as the Schmidt number increases. This is because there is a decrease in the nanoparticle volume fraction boundary layer thickness with the increases in the Schmidt number.

Figure 10 display the influence of chemical reaction parameter k_1 on concentration profile. Concentration decreases with an increase in the chemical reaction parameter indicating that the nanoparticle volume fraction decreases with the increase of chemical reaction parameter. This is because the chemical reaction in this system results in consumption of the chemical and results in decrease of concentration profile.

5. CONCLUSIONS.

Some of the important findings of this observations are given below:

- Increasing Prandtl number decelerates the flow and strongly depresses temperatures throughout the boundary layer regime. while the opposite behavior is seen in case of enhancing the values of Biot (*Bi*) number.
- Concentration is decreased by the Brownian motion parameter,

Schmidt number and reaction parameter.

- As the value of Eckert number (*Ec*) increases, the temperature profiles increase.

- We noticed that concentration profiles first decrease near the sheet surface when the fluid is being heated and situation is completely reversed in the other part of the boundary layer flow.
- Present results are in excellent agreement with the results reported by A. Rauf et al. [23].

ACKNOWLEDGEMENTS

The authors are grateful to Prof. Koneru S. R., Retired Professor, Department of Mathematics, IIT Bombay, India for its support through this paper. Also, the authors thank the reviewers for their constructive suggestions and comments, which have improved the quality of the article considerably.

CONFLICT OF INTEREST

The authors declare that they have no conflict of interest.

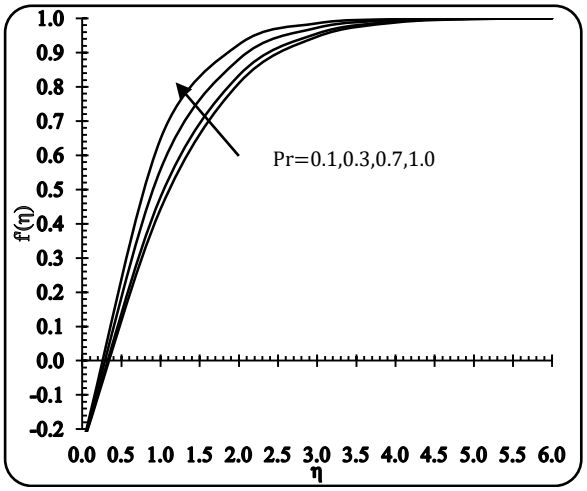

***Figure 1**. Variation in velocity $f'(\eta)$ vs η for different values of M.*

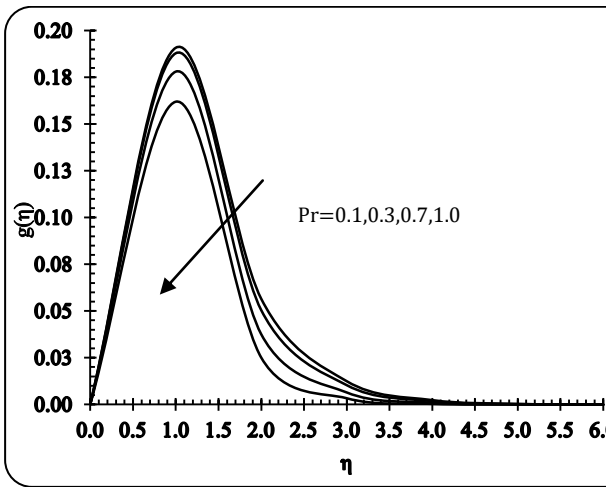

***Figure 2**. Variation in microrotation $g(\eta)$ vs η for different values of M.*

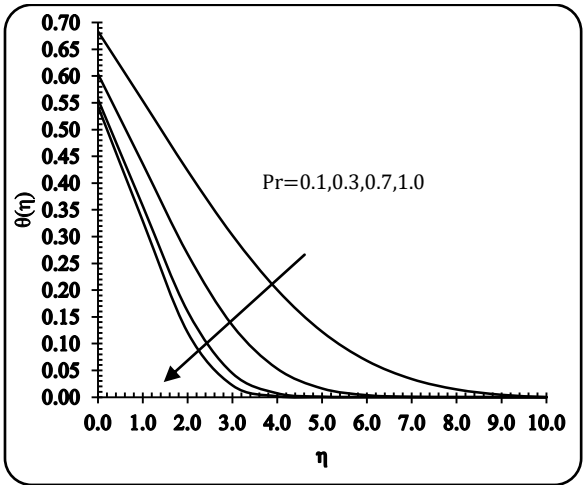

***Figure 3.** Variation in temperature $\theta(\eta)$ vs η for different values of $\Pr$.*

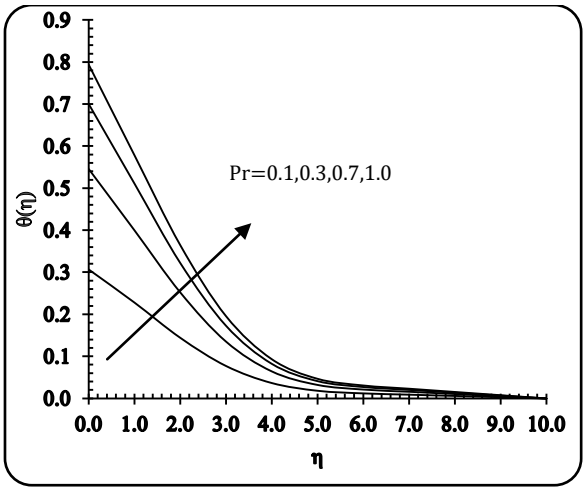

***Figure 4.** Variation in temperature $\theta(\eta)$ vs η for different values of Bi.*

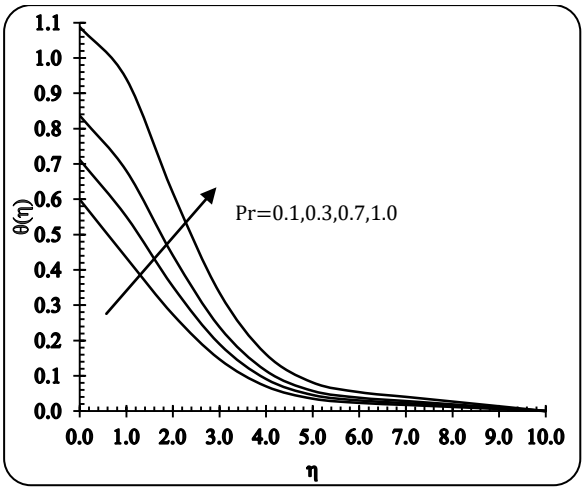

Figure 5. *Variation in temperature* $\theta(\eta)$ *vs* η *for different values of* Ec.

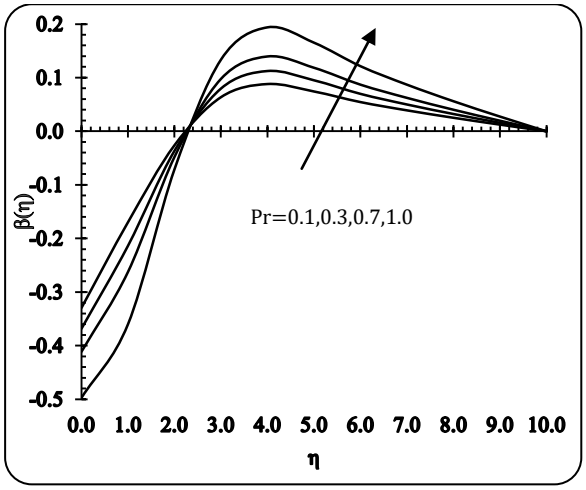

Figure 6. *Variation in concentration* $\beta(\eta)$ *vs* η *for different values of* Ec.

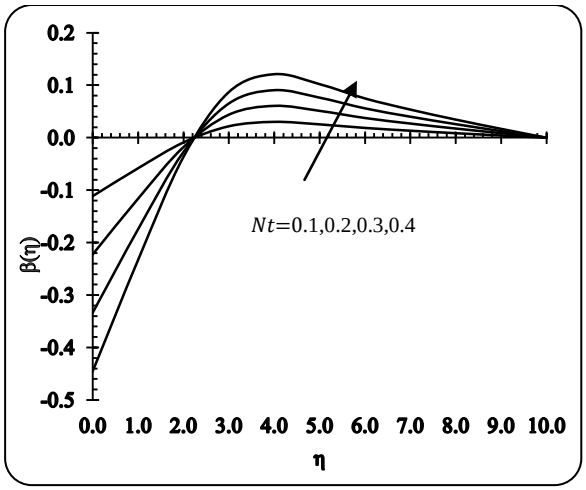

Figure 7. *Variation in concentration* $\beta(\eta)$ *vs* η *for different values of* Nt.

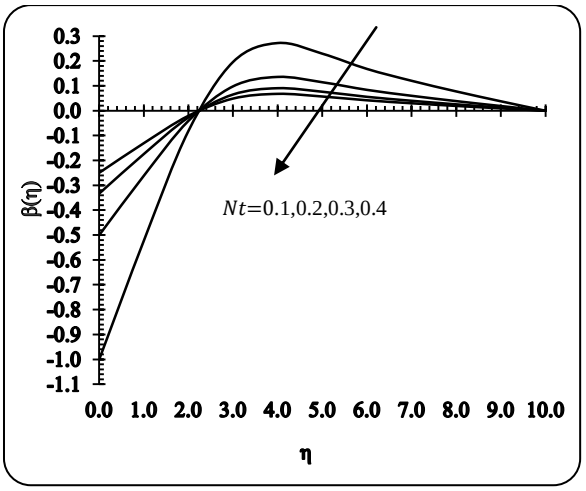

Figure 8. *Variation in concentration* $\beta(\eta)$ *vs* η *for different values of* Nb.

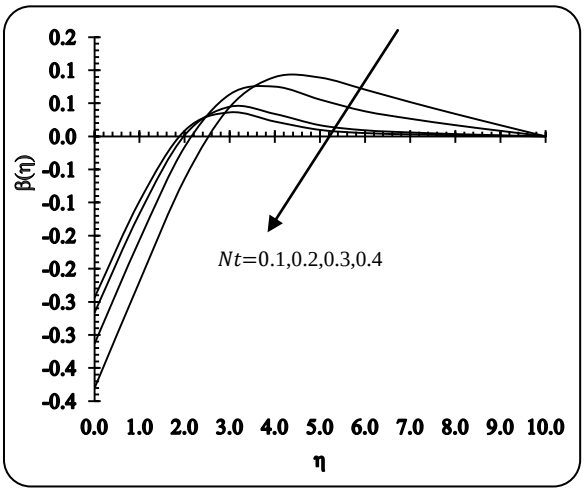

Figure 9. *Variation in concentration* $\beta(\eta)$ *vs* η *for different values of* Sc.

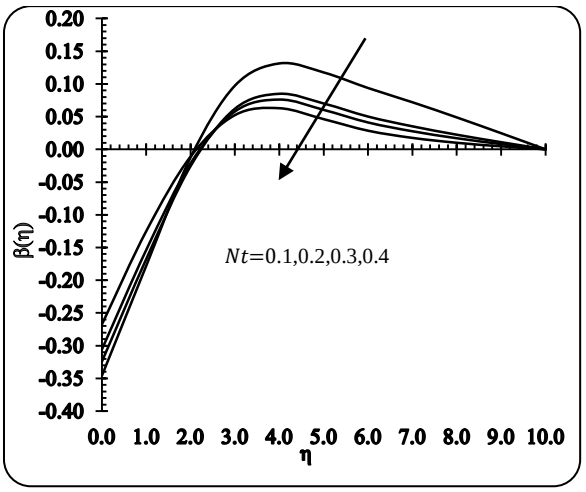

Figure 10. *Variation concentration* $\beta(\eta)$ *vs* η *for different values of* k_1.

REFERENCES

1. Ashraf, M., Bashir, S., "Numerical simulation of MHD stagnation point flow and heat transfer of a micropolar fluid towards a heated shrinking sheet", *Int. J. Numer. Methods Fluids*, 69 (2) (2012) 384–398.
2. Rauf, A., Ashraf, M., Batool, K., Hussain, T., Miraj, M. A., "MHD flow of a micropolar fluid over a stretchable disk in a porous medium with heat and mass transfer", *AIP Adv.*, 5 (2015) 077156.
3. Rashidi, M. M., Ashraf, M., Rostami, B., Rastegari, M. T., Bashir, S., "Mixed convection boundary-layer flow of a micropolar fluid towards a heated shrinking sheet by homotopy analysis method", *Thermal Sci.*, 20 (1) (2016) 21-34.
4. Shehzad, S. A., Waqas, M., Alsaedi, A., Hayat, T., "Flow and heat transfer over an unsteady stretching sheet in a micropolar fluid with convective boundary conditions", *J. Appl. Fluid Mech.*, 9 (3) (2016) 1437–1445.
5. Pal, D., Mandal, G., Vajravelu, K., "Flow and heat transfer of nanofluids at a stagnation point flow over a stretching/shrinking surface in a porous medium with thermal radiation", *Appl. Math. Comput*, 238 (2014) 208–224.
6. Pal, D., Mandal, G., "Influence of thermal radiation of mixed convection heat and mass transfer stagnation-point flow in nanofluids over stretching/shrinking sheet in a porous medium with chemical reaction", *Nuclear Eng. Design*, 273 (2014) 644–652.
7. Hayat, T., Ashraf, M. B., Shehzad, S. A., Alsaedi, A., "Mixed convection flow of Casson nanofluid over a stretching sheet with convectively heated chemical reaction and heat source/sink", *J. Appl. Fluid Mech.*, 8(4) (2015) 803–813.
8. Hayat, T., Imtiaz, M., Alsaedi, A., "MHD 3D flow of nanofluid in presence of convective conditions", *J. Mol. Liq.*, 212 (2015) 203–208.
9. Hayat, T., Farooq, S., Alsaedi, A., Ahmad, B., "Hall and radial magnetic field effects on radiative peristaltic flow of Carreau-Yasuda fluid in a channel with convective heat and mass transfer", *J. Magnet. Magnet. Mater.*, 412 (2016) 207–216.
10. Imtiaz, M., Hayat, T., Alsaedi, A., Ahmad, B., "Convective flow of carbon nanotubes between rotating stretchable disks with thermal radiation effects", *Int. J. Heat Mass Transf.*, 101 (2016) 948–957.
11. Hayat, T., Saeed, Y., Asad, S., Alsaedi, A., "Convective heat and mass transfer in flow by an inclined stretching cylinder", *J. Mol. Liq.*, 220 (2016) 573–580.
12. Sheikholeslami, M., Jafaryar, ZafarSaid, M., Ammar, I., Alsabery, Houman Babazadeh, Ahmad Shafee, "Modification for helical turbulator to augment heat transfer behavior of nanomaterial via numerical approach", *Applied Thermal Engineering*, 182(5) (2021) 115935.
13. Hosseinzadeh, Kh., Erfani Moghaddam, M. A., Asadi, A., Mogharrebi, A. R., Ganji, D. D., "Effect of two different fins (longitudinal-tree like) and hybrid nano-particles $\left(MoS_2 - TiO_2\right)$ on solidification process in triplex latent heat thermal energy storage system", *Alexandria Engineering Journal*, 60(1) (2021) 1967–1979.
14. Hosseinzadeh, Kh., Roghani, S., Mogharrebi, A. R., Asadi, A., Ganji, D. D., "Optimization of hybrid nanoparticles with mixture fluid flow in an octagonal porous medium by effect of radiation and magnetic field", *Journal of Thermal Analysis and Calorimetry*, 143 (2021) 1413–1424.
15. Hosseinzadeh, Kh., Erfani Moghaddam, M. A., Asadi, A., Mogharrebi, A. R., Ganji, D. D., "Effect of internal fins along with Hybrid Nano-Particles on solid process in star shape triplex Latent Heat Thermal Energy Storage System by numerical simulation", *Renewable Energy*, 154 (2020) 497-507.
16. Govardhan, K., Narender, G., Sreedhar Sarma, G., "Heat and Mass transfer in MHD Nanofluid over a Stretching Surface along with Viscous Dissipation Effect", *International Journal of Mathematical, Engineering and Management Sciences*, 5(2) (2020) 343-352.
17. Ramya, D., Rao, J. A., Shravani, I., "Numerical Simulation of MHD Boundary Layer Stagnation Flow of nofluid over aNaStretching Sheet with Slip and Convective Boundary Conditions", *Int. J. Nanosci. Nanotechnol.*, 16(2) (2020) 103-115.
18. Narender, G., Govardhan, K., Sreedhar Sarma, G., "Viscous dissipation and thermal radiation effects on the flow of Maxwell nanofluid over a stretching surface", *Int. J. Nonlinear Anal. Appl.*, 12(2) (2021) 1267-1287.
19. Gangaiah, T., Saidulu, N., Venkata Lakshmi, A., "The Influence of Thermal Radiation on Mixed Convection MHD Flow of a Casson Nanofluid over an Exponentially Stretching Sheet", *Int. J. Nanosci. Nanotechnol.*, 15(2) (2019) 83-98.
20. Ramesh Babu, K., Narender, G., Govardhan, K., "MHD FLOW OF AN EYRING-POWELL FLUID WITH THE EFFECT OF THERMAL RADIATION, JOULE HEATING AND VISCOUS DISSIPATION", *Advances in Mathematics: Scientific Journal*, 9(11) (2020) 9259–9271.
21. Narender, Ganji., Govardhan, Kamatam., Sreedhar Sarma, Gobburu., "Magnetohydrodynamic stagnation point on a Casson nanofluid flow over a radially stretching sheet", *Beilstein J. Nanotechnol.*, 11 (2020) 1303–1315.

22. Ramya, Dodda., Srinivasa Raju, R., Anand Rao, J., Rashidi, M. M., "Boundary layer Viscous Flow of Nanofluids and Heat Transfer Over a Nonlinearly Isothermal Stretching Sheet in the Presence of Heat Generation/Absorption and Slip Boundary Conditions", *Int. J. Nanosci. Nanotechnol.*, 12(4) (2016) 251-268.
23. Rauf, A., Shehzad, S. A., Hayat, T., Miraj, M. A., Alsaedi, A., "MHD stagnation point flow of micro nanofluid towards a shrinking sheet with convective and zero mass flux conditions", *Bulletin of The Polish Academy of Sciences Technical Sciences*, 65(2) (2017) 155-162.